Acta Oceanol. Sin., 2018, Vol. 37, No. 1, P. 30–39
DOI: 10.1007/s13131-018-1156-x
http://www.hyxb.org.cn
E-mail: hyxbe@263.net

Comparison of the Arctic upper-air temperatures from radiosonde and radio occultation observations

CHANG Liang[1, 2], GUO Lixin[1, 2], FENG Guiping[1, 2], WU Xuerui[3, 4], GAO Guoping[1, 2*], ZHANG Yang[5], ZHANG Yu[1, 2]

[1] College of Marine Sciences, Shanghai Ocean University, Shanghai 201306, China

[2] Collaborative Innovation Center for Distant-water Fisheries, Shanghai 201306, China

[3] Shanghai Astronomical Observatory, Chinese Academy of Sciences, Shanghai 200030, China

[4] Key Laboratory of Planetary Sciences, Chinese Academy of Sciences, Shanghai 200030, China

[5] State Key Laboratory of Satellite Ocean Environment Dynamics, Second Institute of Oceanography, State Oceanic Administration, Hangzhou 310012, China

Received 15 November 2016; accepted 13 January 2017

Abstract

The air temperature is one of the most important parameters used for monitoring the Arctic climate change. The constellation observing system for meteorology, ionosphere, and climate and Formosa Satellite Mission 3 (COSMIC/FORMOSAT-3) radio occultation (RO) "wet" temperature product (i.e., "wetPrf") is used to analyze the Arctic air temperature profiles at 925–200 hPa in 2007–2012. The "wet" temperatures are further compared with radiosonde (RS) observations. The results from the spatially and temporally synchronized RS and COSMIC observations show that their temperatures agree well with each other, especially at 400 hPa. Comparisons of seasonal temperatures and anomalies from the COSMIC and homogenized RS observations suggest that the limited number of COSMIC observations during the spatial matchup may be insufficient to describe the small-scale spatial structure of temperature variations. Furthermore, comparisons of the seasonal temperature anomalies from the RS and 5°×5° gridded COSMIC observations at 400 hPa during the sea ice minimum (SIM) of 2007 and 2012 are also made. The results reveal that similar Arctic temperature variation patterns can be obtained from both RS and COSMIC observations over the land area, while extra information can be further provided from the densely distributed COSMIC observations. Therefore, despite COSMIC observations being unsuitable to describe the Arctic temperatures in the lowest level, they provide a complementary data source to study the Arctic upper-air temperature variations and related climate change.

Key words: Arctic temperature, radio occultation, radiosonde

Citation: Chang Liang, Guo Lixin, Feng Guiping, Wu Xuerui, Gao Guoping, Zhang Yang, Zhang Yu. 2018. Comparison of the Arctic upper-air temperatures from radiosonde and radio occultation observations. Acta Oceanologica Sinica, 37(1): 30–39, doi: 10.1007/s13131-018-1156-x

1 Introduction

Arctic air temperature variations play an important role in numerous processes in the Arctic Region by controlling the transfer of mass and moisture fluxes through the lower troposphere. It is therefore essential that the Arctic air temperature is accurately monitored. General circulation models (GCMs) are a feasible way to predict the air temperature at low latitudes, but they appear to under-predict temperatures over the Arctic (Melles et al., 2012; Ballantyne et al., 2013). The operational radiosonde (RS) is a common tool to detect temperature variations in the troposphere and lower stratosphere (e.g., Bohlinger et al., 2014), while it is mainly available over land areas and suffers from poor spatial resolution. Space-borne monitoring is an effective and increasingly important way to obtain temperature profiles with improving accuracy over both land and ocean, which has been demonstrated in the polar regions with moderate resolution imaging spectroradiometer (MODIS) (e.g., Liu and Key, 2003), high resolution infrared radiation sounder (HIRS) (e.g., Liu et al., 2006) and Atmospheric Infrared Sounder (AIRS) data (e.g., Devasthale et al., 2010, 2013), etc. However, these infrared-based sensors are typically sensitive to the presence of clouds, which may limit their applications in the polar regions due to the low frequency of cloud-free conditions in the polar regions (Liu et al., 2012; Chan and Comiso, 2013).

The global navigation satellite system (GNSS) radio occultation (RO) is the first space-borne remote sensing technology that can provide high vertical resolution (less than 1 km) all-weather refractivity profiles, which depend on pressure, temperature and humidity (Kuo et al., 2000; Yunck et al., 1999). The RO technology is based on the time delays of the radio signal propagating from the GNSS satellite (e.g., global positioning system (GPS)) to the receiver placed on a low earth orbit (LEO) satellite (Kursinski et al., 1997). A radio signal is bent by the atmosphere, and the bending angles of the RO signal are derived from the propaga-

Foundation item: The National Basic Research Program (973 Program) of China under contract No. 2015CB953900; the National Natural Science Foundation of China under contract Nos 41506211, 41276197, 41501384, 41606208 and 41706210; the Shanghai Oriental Scholar Program of China under contract No. 2012-58; the Shanghai Sailing Program of China under contract No. 14YF1410200.

*Corresponding author, E-mail: gpgao@shou.edu.cn

tion time, which can be precisely measured with atomic clocks. The retrieved bending angle profiles are used to derive the profiles of refractivity, and subsequently meteorological parameters such as pressure, temperature and humidity (Kuo et al., 2000). It is not possible for the RO technology to separate water vapor and temperature effectively without a priori information, caused by the ambiguity between the temperature and the water vapor in refractivity. As a result, the "dry" temperature can be derived in the stratosphere and upper troposphere where the water vapor partial pressure can be neglected, while the "wet" temperature can be estimated with moisture information included. Considering the RO technology has the advantages of global coverage, high accuracy, long-term stability and self-calibration (Kursinski et al., 1997; Wickert et al., 2001; Hajj et al., 2004), it may offer us a unique opportunity to monitor the state of the Arctic air temperature.

In this paper, the "wet" temperature profiles from the constellation observing system for meteorology, ionosphere, and climate (COSMIC)/Formosa Satellite Mission 3 (hereafter COSMIC) RO observations are used to obtain the Arctic seasonal mean temperatures and anomalies from 2007 to 2012. The COSMIC temperatures and anomalies are then compared with the results from RS observations. This paper is organized as follows. In Section 2, the temperature profiles from the RS and COSMIC observations are compared to understand their characteristics in describing the Arctic atmospheric temperature. In order to understand the characteristics of the RS and COSMIC observations in monitoring the Arctic climate change, Section 3 compares the seasonal mean temperatures and anomalies from spatially matched RS and COSMIC observations, and analyzes their differences between the RS and 5°×5° gridded COSMIC observations. Section 4 is devoted to discussing the temperature anomaly differences from the RS and 5°×5° gridded COSMIC observations during the record minimum sea ice extents of 2007 and 2012, and comparing the performances of the RS and COSMIC observations in revealing the temperature variations during the sea ice minimum (SIM) events. Finally, the conclusions of the present analysis are summarized in Section 5.

2 Analysis of COSMIC derived temperature profiles

2.1 *RO data*

The COSMIC, launched in April 2006, is a joint US/Taiwan GPS RO mission consisting of six identical micro-satellites. The COSMIC mission can provide in near real time the vertical profiles of bending angles, refractivity, temperature, pressure, and water vapor in the neutral atmosphere and electron density in the ionosphere with the global coverage. Therefore, the COSMIC mission can be used for atmospheric and ionospheric research, as well as for improving global weather forecasts and climate change related studies. A distinctive feature of the COSMIC mission, compared with previous RO missions, is tracking both setting and rising neutral atmospheric occultations in an open-loop (OL) mode (Schreiner et al., 2007).

In the present study, the COSMIC post-processed level-2 "wetPrf" product (Das and Pan, 2014) during the period from 13 July 2006 to 31 December 2013 is collected from the COSMIC Data Analysis and Archive Center (CDAAC) for further analysis. The "wetPrf" product, with a priori tropospheric water vapor information included, is generated by one-dimensional variational analysis (1-DVAR). Unlike the "dry" temperatures (i.e., "atmPrf" product), which are known to be of great quality in the upper troposphere and the lower stratosphere (e.g., Kursinski et al., 1997; Hajj et al., 2004; Sun et al., 2013; Kuo et al., 2004), the performance of the "wet" temperatures (i.e., "wetPrf" product) needs to be further investigated. Therefore, the "wet" temperature profiles, rather than the "dry" temperature profiles, are used in this study to compare with the RS temperature measurements at 925–200 hPa over the Arctic. The post-processed version of "wetPrf" data is 2010.2640, and the altitude range is 0–40 km at 100 m vertical resolution.

The spatial distribution of the COSMIC observations from 13 July, 2006 to 31 December, 2013 in the Arctic Region (65°–90°N) are shown on 5°×5°grids (i.e., 72 columns by 5 rows) in Fig. 1. As a

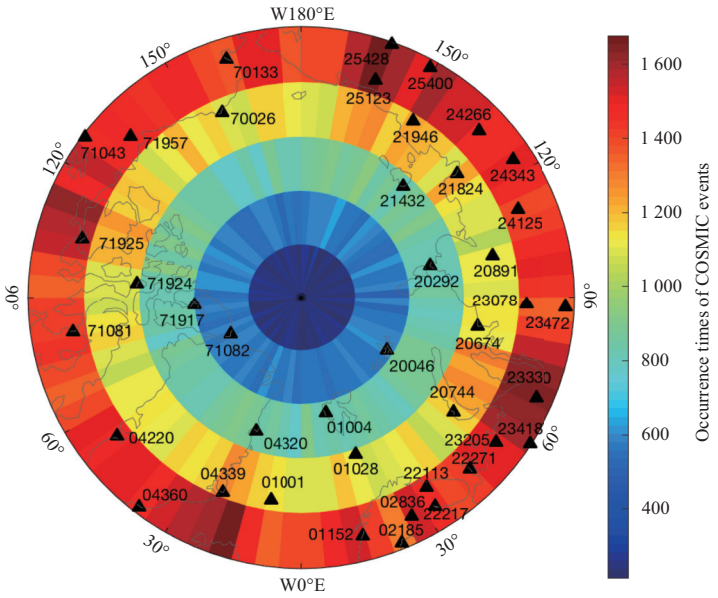

Fig. 1. Spatial distribution of the number of COSMIC observations superimposed on the coastlines of the Arctic Region from 13 July, 2006 to 31 December, 2013. The blue numbers are the World Meteorological Organization (WMO) identifications of RS sites, and the black solid triangles denote the RS sites.

result, a total of 309 102 valid profiles are recorded from 13 July, 2006 to 31 December, 2013, and a maximum of 1 676 profiles in single grid is observed. As illustrated in Fig. 1, the number of COSMIC profiles decreases as the latitude increases in the Arctic, and it was marked with very low coverage over the areas near the North Pole (80°–90°N). One of the most probable reasons for the diminishing number of COSMIC profiles might be the decreasing area of the grid cells closer to the North Pole.

2.2 *RS observations*

Despite the low spatial resolution of the RS observations, they are a key data set in operational weather forecasting and upper-air climate research (Sun et al., 2010). Furthermore, the high-quality RS observations are also very valuable for the calibration and validation of satellite temperature (e.g., Sun et al., 2010) and water vapor retrievals (e.g., Chang et al., 2015). The integrated global radiosonde archive (IGRA) is a quality-controlled compilation of the RS observations from the global network of more than 1 500 stations and includes the observed temperature, geopotential height, humidity, wind direction, and wind speed at standard (mandatory) pressure levels and significant levels (Durre et a., 2006). In this study, the RS temperature profiles from 925 to 200 hPa extracted from IGRA are used to compare with the COSMIC temperature profiles. Given that the values of the geopotential height or temperature at some pressure levels are not recorded from time to time, the RS data levels in the absence of either geopotential height or temperature are removed during processing.

2.3 *Comparison of RS and COSMIC Arctic temperature profiles*

In this study, the RS- and COSMIC-derived temperature profiles are compared over the Arctic. The horizontal distance is limited to within 100 km and the time window is 2 h during the matchup process between the RS and COSMIC observations. In addition, given that the lowest altitude of only 0.1 km can be reached for the COSMIC temperature profiles, the temperature comparisons are made at the standard pressure levels of the RS profiles from 925 to 200 hPa only (i.e., 925, 850, 700, 600, 500, 400, 300, 250 and 200 hPa, respectively), excluding the 1 000 hPa and surface levels. Moreover, considering the vertical resolution of the COSMIC profiles is much higher than the RS standard pressure levels, the COSMIC temperature profiles are interpolated in the standard pressure levels of the RS profiles (Wang et al., 2013) via

$$\alpha=\frac{\ln p-\ln p_2}{\ln p_1-\ln p_2},\quad \beta=\frac{\ln p_1-\ln p}{\ln p_1-\ln p_2}, \tag{1}$$

$$T=\alpha T_1+\beta T_2, \tag{2}$$

where p and T are the pressure and temperature at the standard pressure level; p_i and T_i (i = 1, 2) represent the pressure and temperature from COSMIC "wetPrf", respectively.

Figure 2 shows the scatterplots of temperatures between the COSMIC and all available Arctic RS observations at the standard pressure levels from 925 to 200 hPa during the period from 13 July, 2006 to 31 December, 2013. Despite the correlation coefficients between the RS and COSMIC temperatures are all greater than 0.96 at each level (Fig. 2), the root mean square (RMS) values of the temperature differences between the RS and COSMIC observations are non-uniform from 925 to 200 hPa. The RMS decreases from 2.04°C at 925 hPa to 1.51°C at 400 hPa, while it increases to 1.74°C at 200 hPa. Therefore, a large discrepancy between the RS and COSMIC temperature is observed at the lower and upper levels, and a minimum RMS of 1.51°C is detected at 400 hPa. The above temperature differences at the lower levels may be explained by the significant systematic negative bias (N-bias) remains in derived refractivity profiles in the atmospheric boundary layer (ABL) (e.g., Xie et al., 2010). Moreover, there are significant representativeness errors between the two types of soundings since the RS is a series of point measurements that drift as they ascend through the atmosphere, whereas the COSMIC actually measures the averages over finite volumes (on the order of 300 km) of the atmosphere (Kuo et al., 2004; Anthes, 2011).

3 Arctic seasonal mean temperature and anomaly profiles from the RS and COSMIC observations in 2007–2012

The value of operational RS observations for climate monitoring is strongly hindered by numerous and poorly documented changes in instrumentation and operational procedures (Titchner et al., 2009). In addition, differences between radiosondes from different manufacturers complicated the comparison of data records from different sources (Moradi et al., 2013). Therefore, it may be arbitrary to use the RS records directly for long-term climate monitoring and trend detection. An effective way to estimate the mean temperature variations over the Arctic is to remove the inhomogeneities in the RS data. In this Section, the seasonal mean temperatures and anomalies from the COSMIC and homogenized RS data are investigated, and used to compare the abilities of the COSMIC and homogenized RS data in revealing Arctic temperature changes. Considering only an average of about 13 spatio-temporally synchronized matchups (not shown) between the RS and COSMIC temperature profiles at 925 hPa is obtained per single RS site during the period from 13 July, 2006 to 31 December, 2013, the abilities of the COSMIC observations in characterizing the Arctic temperature variations may need to be further investigated, since the COSMIC observations are more widely distributed than the RS observations in spatial domains. Unlike the temperature comparisons made in Section 2, where the measurements are matched both temporally and spatially, another two schemes were designed in this Section. It is important to note that the homogenized RS data used in the rest of the paper are generated with updated radiosonde observation correction using reanalyses (RAOBCORE) (Haimberger, 2007) and radiosonde innovation composite homogenization (RICH) software packages (Haimberger et al., 2012) to remove the inhomogeneity errors due to the irregular distribution of RS stations and constant changes of instruments in space and time. The homogenized RS products from RAOBCORE and RICH software packages are generated with a global radiosonde temperature data set back to 1958, which have been verified with temperature data set based on advanced microwave sounding unit (AMSU) radiances (Haimberger et al., 2012).

(1) Scheme I: The seasonal mean temperatures and anomalies during 2007–2012 over the study area are first obtained from all available homogenized RS observations, which are further compared with those derived by spatially synchronized COSMIC observations. In this scheme, a time window of 2 h is eliminated during the matching process between the RS and COSMIC observations, and all COSMIC observations in a circle of radius 100 km at each RS site are used.

(2) Scheme II: The seasonal mean temperatures and anomalies from the homogenized RS observations in Scheme II are obtained as in Scheme I. However, the seasonal mean temperat-

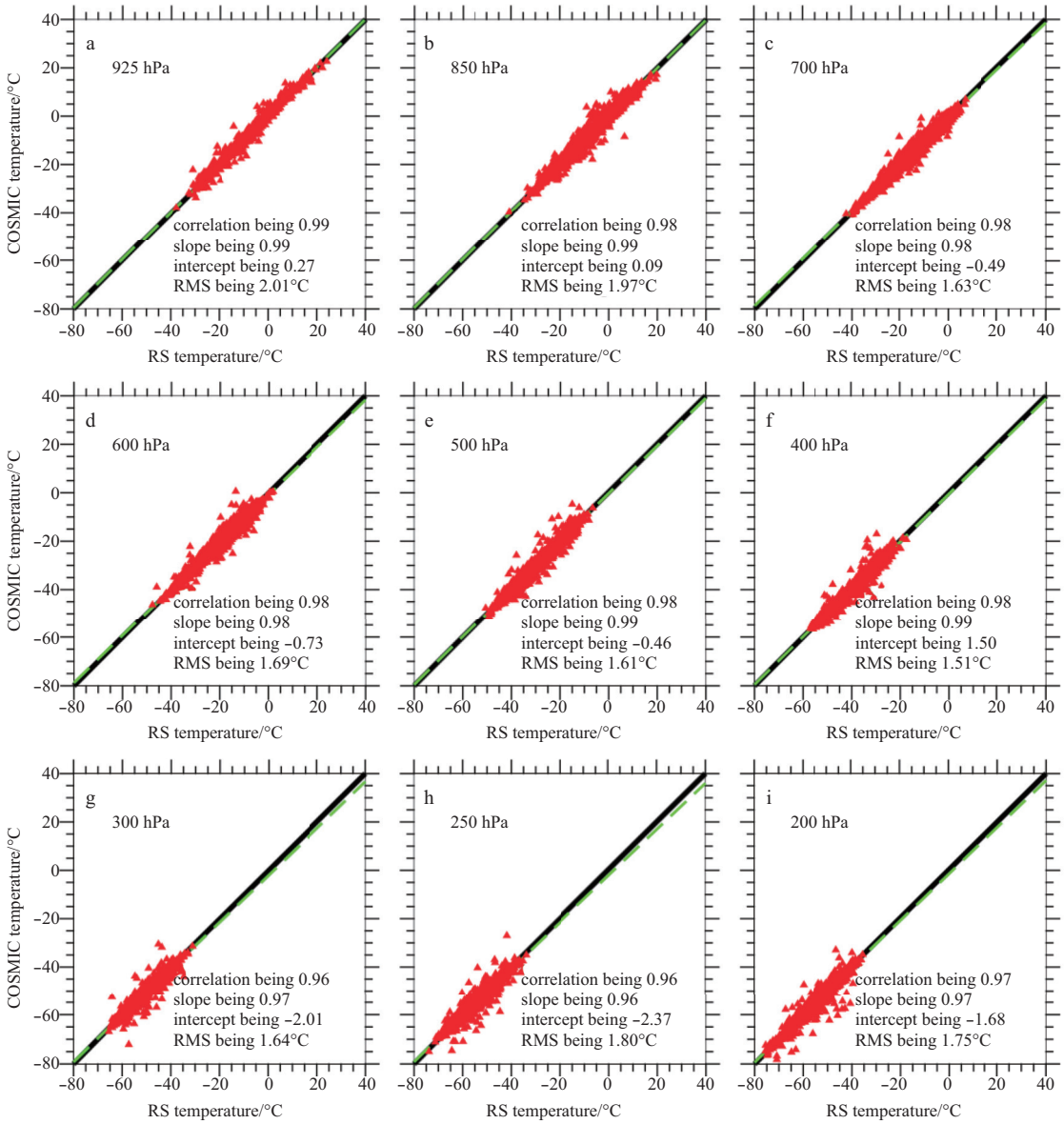

Fig. 2. Scatter plots of Arctic mean temperature profiles between RS and COSMIC observations at different pressure levels from 925 to 200 hPa. The linear regression is shown as the green dashed line, and the black line is the zero bias.

ures and anomalies from the COSMIC observations are generated at 5°×5° grids for each standard level at 925–200 hPa in 2007–2012. In this scheme, the original temporal (i.e., a time window of 2 h) and spatial (i.e., a circle of radius 100 km) limitations during the matching process in Scheme I are both extended, and the gridded COSMIC observations are compared with the spatially located RS data.

3.1 *Seasonal mean temperature profiles from 2007 to 2012 in the Arctic*

In Fig. 3, the seasonal mean temperature profile differences between the spatially synchronized RS and COSMIC observations (i.e., Scheme I) at 925–200 hPa in 2007–2012 over the Arctic are shown. It should be noted that 3 month seasons are defined as March–May (spring), June–August (summer), September–November (autumn) and December to the following February in the next year (winter). It is clear in Fig. 3 that the seasonal mean temperature differences are still remarkable at the low levels after increasing the number of COSMIC observations in the time domain, especially for the bottom level of 925 hPa. The mean temperature differences are less than about ±1.0°C at 850–200 hPa at all seasons except the autumn seasons of 2010 and 2011. The RMS and mean difference (MD) of the seasonal temperature and anomaly at 925–200 hPa between the RS and COSMIC observations in Schemes I in 2007–2012 are listed in Table 1. As we can see in Table 1, the RMS values in Schemes I are less than 0.6°C at all levels except for a RMS of 1.32°C observed at 925 hPa. The best agreement is achieved at 300 hPa with a RMS of 0.32°C, followed by 250 and 400 hPa (i.e., a RMS of 0.40°C and 0.42°C, respectively). In addition, the MDs between the RS and COSMIC observations in Scheme I are within ±0.14°C at 925–200 hPa except for a MD of −0.32°C detected at 700 hPa.

Considering that the RO events are globally quasi-random distributed, the number of COSMIC observations matched around the RS sites is still rather low. In order to assimilate more COSMIC observations during the comparison, the COSMIC data

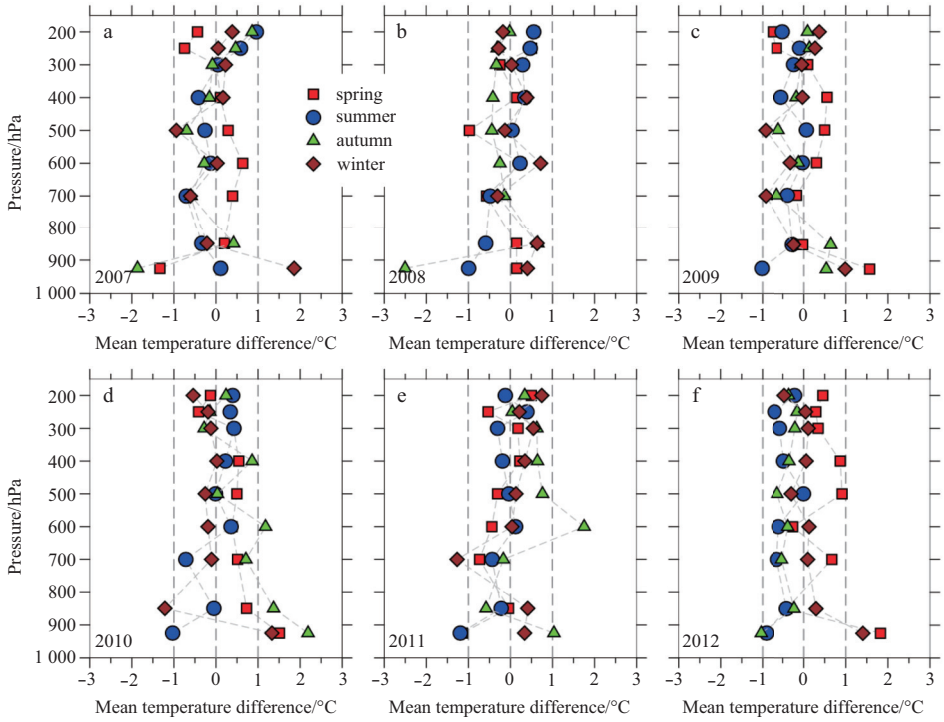

Fig. 3. The differences of Arctic mean temperature profiles at 925–200 hPa between RS and COSMIC observations in Scheme I in each season from 2007 to 2012.

Table 1. The RMS and MD of the seasonal mean temperature and anomaly differences at 925–200 hPa between the RS and COSMIC observations in 2007–2012

Pressure level/hPa	Temperature/°C				Temperature anomaly/°C			
	Scheme I (Fig. 3)		Scheme II (Fig. 4)		Scheme I (Fig. 5)		Scheme II (Fig. 6)	
	RMS	MD	RMS	MD	RMS	MD	RMS	MD
925	1.32	0.09	1.47	–1.25	1.03	0.15	0.36	0.08
850	0.54	0.03	1.09	–1.05	0.42	–0.03	0.30	0.03
700	0.59	–0.32	1.02	–0.99	0.41	–0.05	0.23	0.06
600	0.54	0.13	0.72	–0.66	0.46	0.02	0.21	0.06
500	0.52	–0.14	0.84	–0.81	0.49	0.02	0.20	0.07
400	0.42	0.12	0.71	–0.67	0.33	0.13	0.19	0.07
300	0.30	0.04	0.48	–0.40	0.44	0.08	0.25	0.04
250	0.40	–0.02	0.35	0.03	0.58	0.01	0.37	0.06
200	0.49	0.12	0.56	0.24	0.62	0.05	0.43	–0.004

are collected at 5°×5° grids at the region of interest (ROI) for further comparison. The comparison of seasonal mean temperature profiles from the RS and COSMIC observations (i.e., Scheme II) is illustrated in Fig. 4. The seasonal mean temperatures from the COSMIC observations at 5°×5° grids appear to be systemically colder than those from the RS observations in 2007–2012, which is especially obvious at the bottom levels of 925–700 hPa in all seasons except winters. The seasonal mean temperature differences become weaker for the levels of 600–200 hPa, and a minimum RMS of about 0.35°C and an absolute minimum MD of 0.03°C are both observed at 250 hPa (Table 1), respectively.

Comparison of the results of the seasonal mean temperature profiles at 925–200 hPa from the RS and COSMIC observations in Figs 3–4 suggests that larger RMS and MD are detected at almost all levels in Scheme II compared with Scheme I (Table 1). The discrepancy in Scheme II is understandable because the two observations are not spatially synchronized, i.e., the average temperature from the COSMIC data is taken over an area of 5°×5° rather than over the locations of the RS sites. Therefore, it could be concluded that the quasi-random distributed COSMIC observations may be insufficient to describe the small-scale spatial structure of the mean temperature variations.

3.2 *Seasonal temperature anomalies from 2007 to 2012 in the arctic*

In this subsection, the seasonal temperature anomaly profiles at 925–200 hPa from the RS and COSMIC data are compared. The temperature anomalies are defined by a departure from a reference value or long-term average, and calculated as the difference between the long-term average temperature and the temperature that is actually occurring. For example, the temperature anomaly for the summer of 2007 is obtained by subtracting the mean temperature profile of the summer months of 2008–2012 from the mean temperature profile calculated for the summer of 2007. In Fig. 5, the Arctic seasonal temperature anomaly differences between spatially synchronized RS and COSMIC

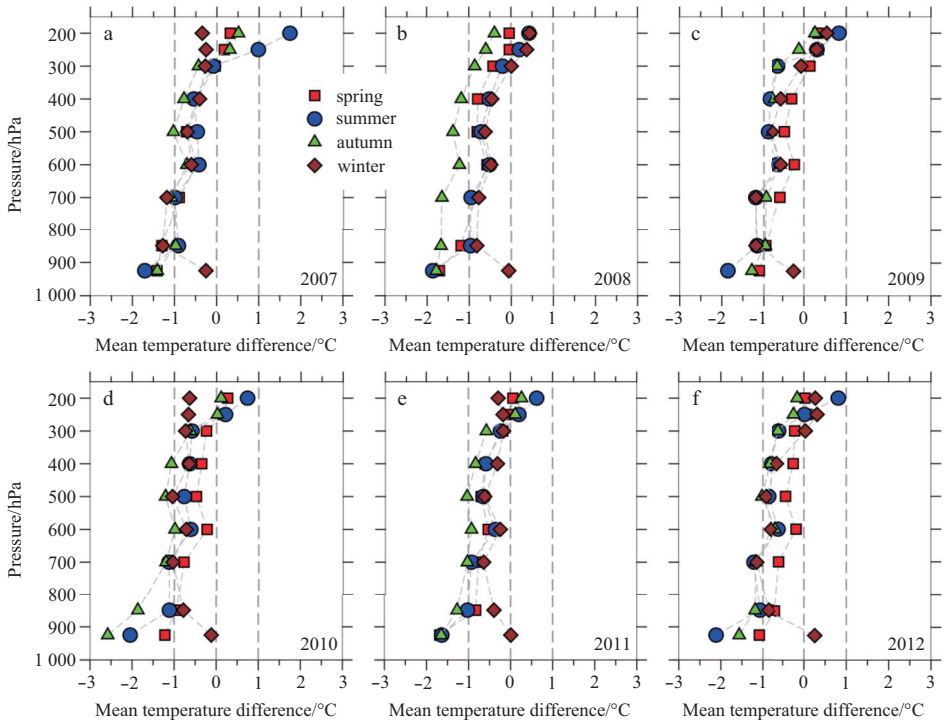

Fig. 4. The differences of Arctic mean temperature profiles at 925–200 hPa between RS and COSMIC observations in Scheme II in each season from 2007 to 2012.

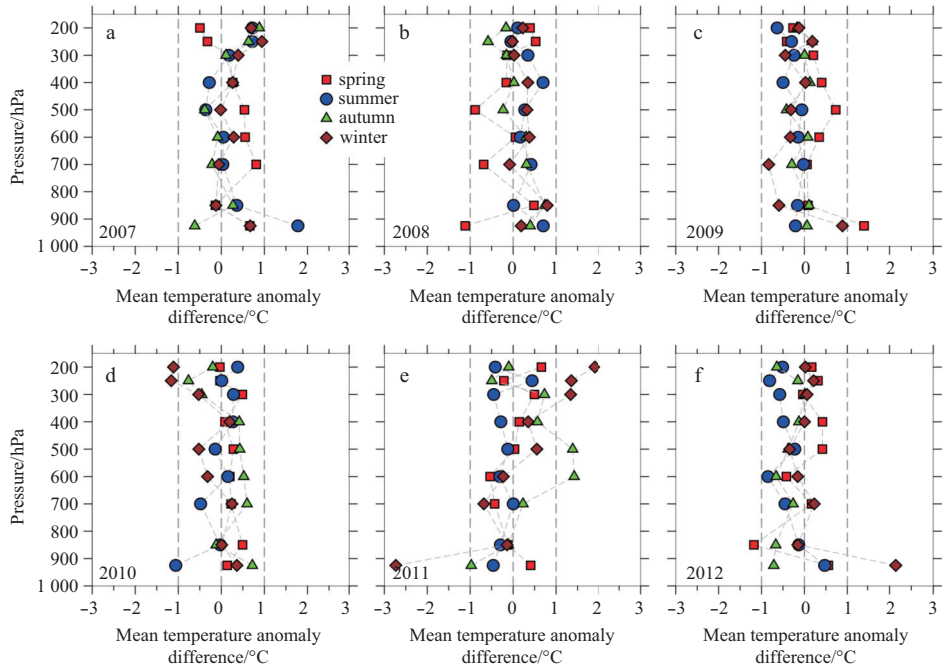

Fig. 5. The differences of the Arctic temperature anomalies at 925–200 hPa between RS and COSMIC observations in Scheme I in each season from 2007 to 2012.

observations (i.e., Scheme I) at 925–200 hPa of 2007–2012 are shown in Fig. 5. The Arctic seasonal temperature anomaly differences from the above two observations showed a large discrepancy at 925 hPa, while consistent results are generally observed with a RMS of less than 0.62°C for the levels above 925 hPa, and the MDs ranged from –0.05 to 0.15°C at all levels (Table 1). However, the anomalies from the spatially synchronized COSMIC observations are not stable enough to explain the temperature anomalies at the locations of the RS sites, since large variations are observed at different levels for the seasons of 2007–2012. Taking the winter of 2011 as an example, a negative anomaly difference of –2.7°C is found at 925 hPa, while a positive anomaly difference of 1.9°C is observed at 200 hPa. Therefore, the number of spatially synchronized COSMIC observations within

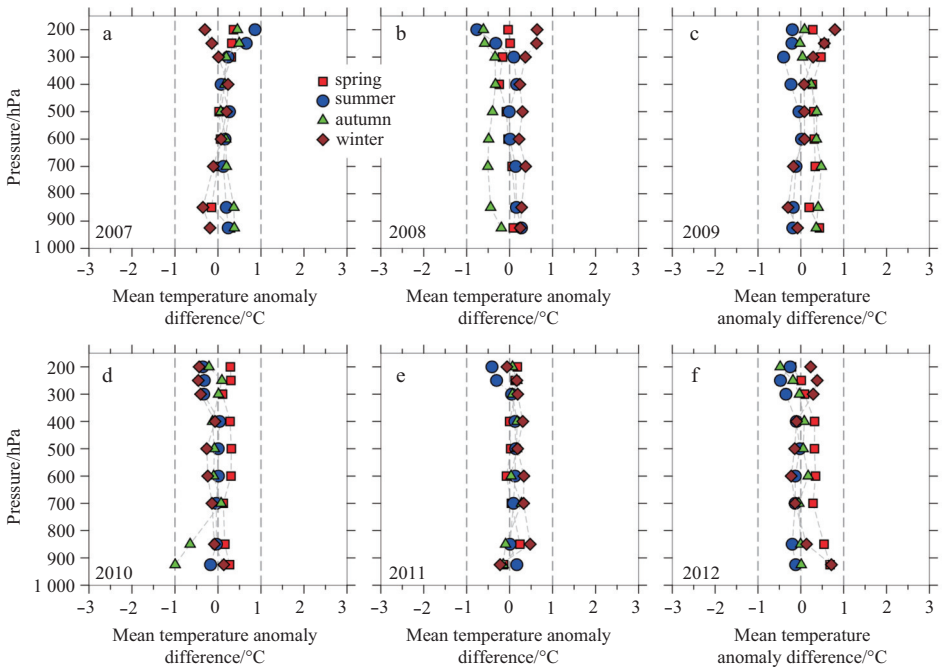

Fig. 6. The differences of the Arctic temperature anomalies at 925–200 hPa between RS and COSMIC observations in Scheme II in each season from 2007 to 2012.

only a circle of radius 100 km may be insufficient to describe the temperature anomalies.

To evaluate the ability of the COSMIC observations for use in the temperature anomaly estimation, the comparison of the arctic seasonal temperature anomalies is also made (Fig. 6) according to Scheme II. As illustrated in Fig. 6, the temperature anomaly differences are less than about ±1.0°C at all levels for all seasons from 2007 to 2012, and those anomalies show better agreement than the results in Fig. 5. Few fluctuations of the seasonal temperature anomaly differences are detected, with the RMS values of seasonal anomaly differences less than 0.43°C, and MDs within the range of –0.004–0.08°C at all levels (Table 1). The RMS values of the seasonal anomaly differences are even lower than 0.30°C at 850–300 hPa, in contrast to a minimum RMS of 0.33°C shown in Fig. 5. Furthermore, at the level of 400 hPa, the smallest seasonal temperature anomaly difference from the RS and COSMIC observations in Scheme II is observed.

4 Seasonal temperature anomalies at 400 hPa from RS and COSMIC observations during 2007 and 2012

The Arctic warming in recent years has been accompanied by a rapid loss of sea ice, especially during the summer season, which has drawn a lot of attention (e.g., Devasthale et al., 2010, 2013; Kay et al., 2011; Kim et al., 2014; Stroeve et al., 2014). It has been reported using both modeling and observational approaches that, the long-term changes in the Arctic sea ice and the several SIM events for the 2000s (e.g., the 1st and 2nd lowest arctic sea ice extents in 2012 and 2007, respectively) were associated with the combined influences of clouds, radiation, circulation, atmospheric preconditioning and ice-albedo feedback, etc. In this section, we compare the Arctic seasonal temperature anomalies at 400 hPa derived from the RS and COSMIC observations during the record minimum sea ice extents of 2007 and 2012, and discussed the performance of the RS and COSMIC observations in revealing the Arctic temperature variations during the SIM events.

The seasonal temperature anomalies from the COSMIC observations at 5°×5°grids (i.e., Scheme II) match well with those from the homogenized RS observations at the pressure level of 400 hPa. Therefore, the following analyses of the Arctic seasonal temperature anomalies during 2007 and 2012 are presented at 400 hPa only. It should be noted that our choice was also consistent with previous reports that the Arctic warming signal is observed from the surface up to 400 hPa (Devasthale et al., 2010, 2013). The spatial distributions of the Arctic seasonal temperature anomalies at 400 hPa in 2007 from the RS and COSMIC observations as well as their differences are shown in Fig. 7. The derived anomalies from the two observations showed similar distributions at all RS sites for the seasons in 2007. Despite a maximum negative and positive anomaly difference of –2.76 and 2.97°C observed in the winter of 2007, the overall temperature anomaly difference is about only 0.11, 0.08, 0.16 and 0.23°C in all seasons, respectively. While the RS observations can describe the temperature anomalies over the land areas only, the temperature anomaly distributions from the COSMIC observations at 5° spatial resolution revealed increased details about the state of the Arctic atmosphere. Taking the temperature anomalies in the summer of 2007 as example, conspicuous positive anomalies are detected from the COSMIC observations over the East Siberian Sea and the Beaufort Sea, which was consistent with the analysis from AIRS data (Devasthale et al., 2010) and may be one of the most important reasons for the SIM of the autumn of 2007. However, no prominent warming signal is observed by coastal RS sites, and only moderate positive anomalies are found at Barrow, USA (71.3°N, 156.8°W) and Cherskiy, Russia (68.8°N, 161.3°E). Therefore, the spatially scattered RS observations over the land may fail to depict the details of the Arctic temperature variations.

In Fig. 8, a comparison of the seasonal temperature anomalies in 2012 at 400 hPa from the RS and COSMIC observations are illustrated. The anomalies from those observations show

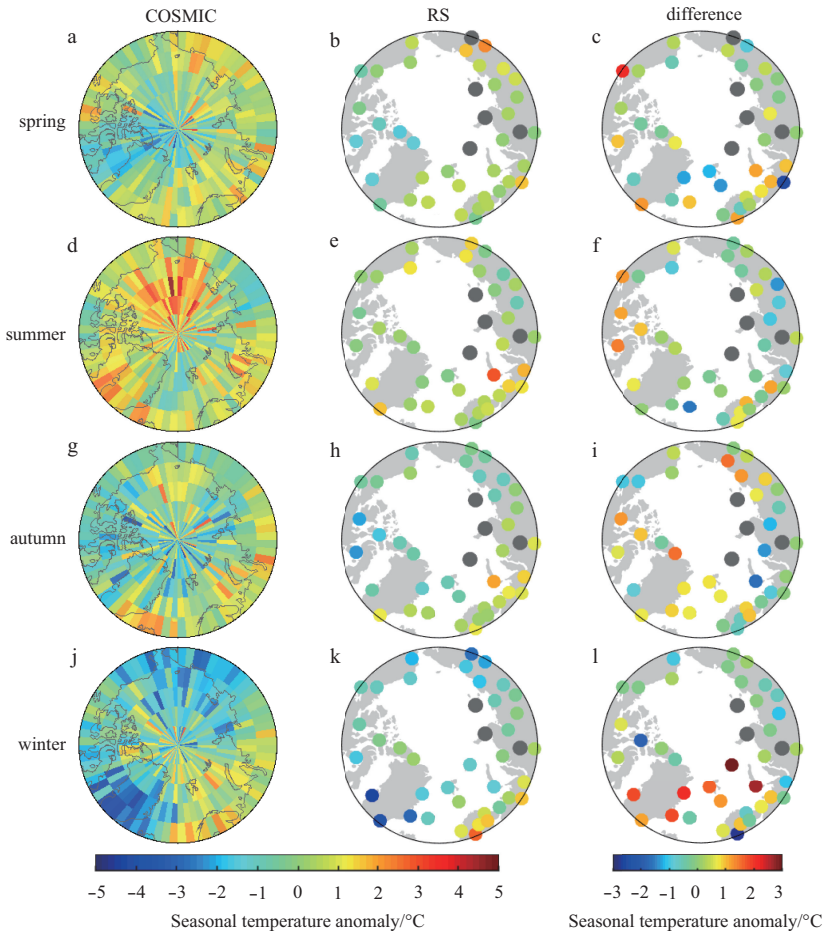

Fig. 7. The horizontal distributions of seasonal temperature anomalies superimposed on the Arctic coastlines from the COSMIC (left column) and RS (middle column) observations in Scheme II, as well as their differences (right column) at 400 hPa in 2007. Note that the grey dots in the middle and right columns are due to missing data at the RS sites.

good consistency in 2012, with the overall mean anomaly difference of only 0.32, –0.11, 0.08 and –0.10°C in each season, respectively. Moreover, the positive anomalies appear to be wider in the spring of 2012 (Fig. 8a) than in the spring of 2007 (Fig. 7a), and the negative anomalies appear to be weaker in spring 2012 than in spring 2007, which are consistent with the analysis from the AIRS data in Devasthale et al. (2013) and could result in the advanced sea ice melt in the spring of 2012. The anomalies from the RS observations shown in Fig. 8b reveal the positive signal in Greenland, Longyearbyen and Franz Josef Land, they however provide little information about the temperature variations over the ocean areas. During the autumn of 2012, the warming signal from the COSMIC observations are detected over oceans such as the Baffin Bay, the Chukchi Sea, the East Siberian Sea, the Laptev Sea and the Kara Sea (Fig. 8g), while the positive anomalies from the RS observations are only observed over land areas including Alaska, Far East of Russia, East Siberia and southern Greenland (Fig. 8h). From both RS and COSMIC observations, although it is found that the positive anomalies in autumn are wider and stronger than those in summer, which play an important role in preventing sea ice build-up in the autumn of 2012 as reported from the AIRS data in Devasthale et al. (2013), less guidance from the RS observations is obtained due to their poor spatial resolution. Therefore, despite the anomalies from the COSMIC and homogenized RS data presenting similar patterns over the land area, the wider coverage of the COSMIC observations shows advantages of revealing the temperature variations over both land and ocean areas, which could be helpful to understand more details about the Arctic climate change.

5 Conclusions

The Arctic air temperature variations play an important role in the Arctic climate change and related processes. In this paper, comparisons of the Arctic air temperature profiles at 925–200 hPa from the RS and COSMIC observations have been conducted. Moreover, the Arctic seasonal mean temperature and anomaly differences from the COSMIC and homogenized RS observations are analyzed to understand the ability of the two observations in monitoring the changes in the Arctic air temperature. Furthermore, the Arctic seasonal temperature anomalies from the COSMIC and homogenized RS observations during 2007 and 2012 are compared to investigate the ability of the COSMIC observations in revealing the temperature variations during the SIM events. Our findings from this study can be summarized as follows.

(1) The comparison of the RS- and COSMIC-detected temperature profiles at 925–200 hPa shows that their correlation coefficients are all greater than 0.96 at each level, while the RMS values of the temperature differences between the RS and COSMIC observations are non uniform from 925 to 200 hPa. The temperature differences from the RS and the COSMIC may result from

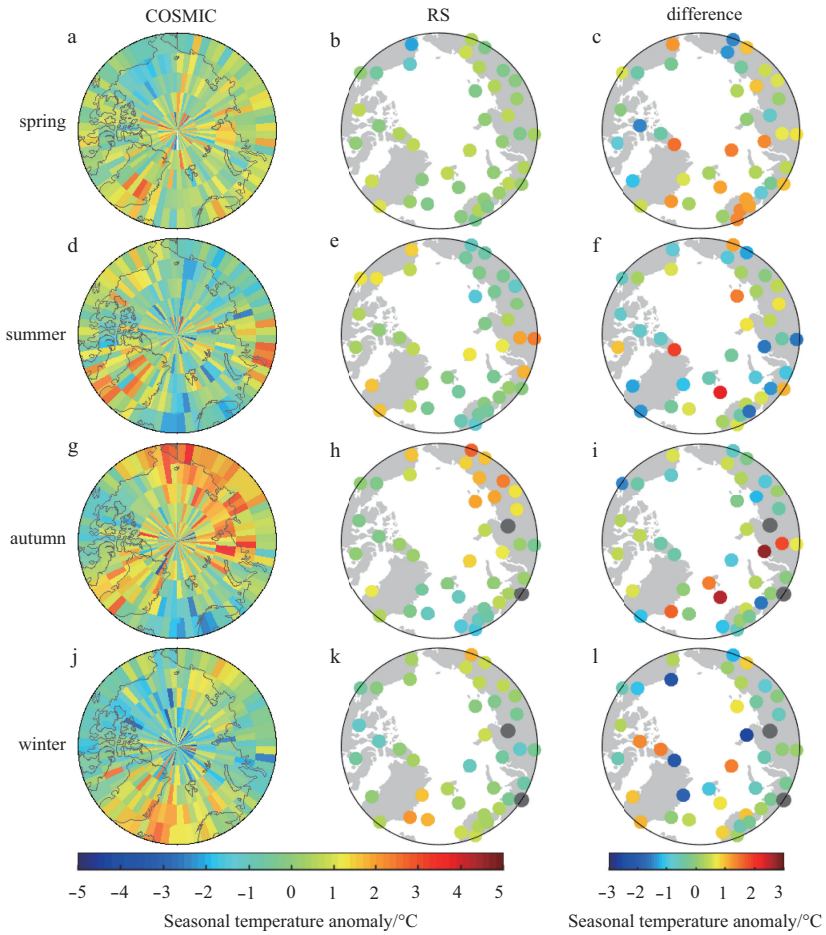

Fig. 8. The horizontal distributions of seasonal temperature anomalies superimposed on the Arctic coastlines from the COSMIC (left column) and RS (middle column) observations in Scheme II, as well as their differences (right column) at 400 hPa in 2012.

their spatial and temporal mismatch and systemic errors of the COSMIC observations. In addition, large temperature discrepancies between the RS and COSMIC observations are observed at the lower and upper levels, while a minimum RMS of 1.51°C was detected at 400 hPa.

(2) The comparison of the seasonal mean temperature and anomaly from the COSMIC and homogenized RS observations in Scheme I shows that despite the mean temperature and anomaly differences from the two observations being generally less than ±1.0°C at 850–200 hPa for all the seasons in 2007–2012, the large variations of those differences are observed at different levels. In contrast, the mean temperature and anomaly difference comparisons exhibited more stable performance at different levels in Scheme II than in Scheme I. The comparison of the seasonal mean temperatures in Scheme II suggests that the spatially synchronized COSMIC observations around the RS sites may be insufficient to describe the small-scale spatial structure of the temperature variations. Moreover, the comparisons of the seasonal temperature anomalies in Scheme II indicate that the 5°×5°gridded COSMIC observations are able to provide stably estimates of the seasonal Arctic temperature anomalies, with a RMS of less than 0.43°C at 925–200 hPa compared with the results from the homogenized RS observations.

(3) The comparison of the Arctic seasonal temperature anomaly distributions from RS and 5°×5° gridded COSMIC observations at 400 hPa in Scheme II during the SIM of 2007 and 2012 shows that the COSMIC temperature anomalies can provide more details about the Arctic temperature variations. As such, the monitoring of atmospheric preconditioning with the RO observations could be a complementary source of information in understanding the Arctic upper-air temperature variations and related climate change.

It is worth mentioning that despite the sparsely distribution of the COSMIC profiles over the inner Arctic Region, incorporation of several other RO missions such as SAC-C (scientific application satellite-C), challenging mini-satellite payload (CHAMP), gravity recovery and climate experiment (GRACE), meteorological operational satellite program (MetOp)-A/B, TerraSAR-X and Korea multi-purpose satellite-5 (KOMPSAT-5) could be helpful to relieve this shortcoming. In addition, the increasing number of future RO missions may be also helpful (e.g., COSMIC II, climate community initiative for continuing earth radio occultation (CICERO), meteorological operational satellite programme (MetOp)-C and Spain's PAZ). Furthermore, with the development of other GNSS (e.g., Russia's GLONASS, Europe's GALILEO and China's Beidou), more RO observations will be available, which will be more beneficial to the understanding of the Arctic climate change.

It should also be noted that despite the validation in this study of the performance of the RO temperatures at 400 hPa in revealing the thermodynamic state of the Arctic atmosphere via comparisons with those from the RS observations, the RO obser-

vations fail to provide sufficient credible clues at the surface atmosphere due to the N-bias in the ABL. The state of the Arctic surface atmosphere, however, is one of the most important issues to understand the interactions between the atmosphere and sea-ice, and thus the Arctic climate feedbacks. Therefore, other information is recommended to be accompanied with the RO observations to further study the Arctic climate change, which would be an important issue in the future.

Acknowledgements

The authors thank Haimberger Leopold (University of Vienna) for providing us with the RAOBCORE and RICH adjusted RS data and Boucher Jason (Northeast Fisheries Science Center, National Oceanic and Atmospheric Administration) for his advices on English grammar and expressions. They are grateful to the COSMIC Data Analysis and Archive Center (CDAAC) and Integrated Global Radiosonde Archive (IGRA) for providing their data.

References

Anthes R A. 2011. Exploring earth's atmosphere with radio occultation: contributions to weather, climate and space weather. Atmospheric Measurement Techniques, 4(6): 1077–1103

Ballantyne A P, Axford Y, Miller G H, et al. 2013. The amplification of arctic terrestrial surface temperatures by reduced sea-ice extent during the Pliocene. Palaeogeography, Palaeoclimatology, Palaeoecology, 386: 59–67

Bohlinger P, Sinnhuber B M, Ruhnke R, et al. 2014. Radiative and dynamical contributions to past and future arctic stratospheric temperature trends. Atmospheric Chemistry and Physics, 14(3): 1679–1688

Chan M A, Comiso J C. 2013. Arctic cloud characteristics as derived from MODIS, CALIPSO, and CloudSat. Journal of Climate, 26(10): 3285–3306

Chang Liang, Gao Guoping, Jin Shuanggen, et al. 2015. Calibration and evaluation of precipitable water vapor from MODIS infrared observations at night. IEEE Transactions on Geoscience and Remote Sensing, 53(5): 2612–2620

Das U, Pan C J. 2014. Validation of FORMOSAT-3/COSMIC level 2 "atmPrf" global temperature data in the stratosphere. Atmospheric Measurement Techniques, 7(3): 731–742

Devasthale A, Sedlar J, Koenigk T, et al. 2013. The thermodynamic state of the arctic atmosphere observed by AIRS: comparisons during the record minimum sea ice extents of 2007 and 2012. Atmospheric Chemistry and Physics, 13(15): 7441–7450

Devasthale A, Willén U, Karlsson K G, et al. 2010. Quantifying the clear-sky temperature inversion frequency and strength over the Arctic Ocean during summer and winter seasons from AIRS profiles. Atmospheric Chemistry and Physics, 10(12): 5565–5572

Durre I, Vose R S, Wuertz D B. 2006. Overview of the integrated global radiosonde archive. Journal of Climate, 19(1): 53–68

Haimberger L. 2007. Homogenization of radiosonde temperature time series using innovation statistics. Journal of Climate, 20(7): 1377–1403

Haimberger L, Tavolato C, Sperka S. 2012. Homogenization of the global radiosonde temperature data set through combined comparison with reanalysis background series and neighboring stations. Journal of Climate, 25(23): 8108–8131

Hajj G A, Ao C O, Iijima B A, et al. 2004. CHAMP and SAC-C atmospheric occultation results and intercomparisons. Journal of Geophysical Research: Atmospheres, 109(D6): D06109

Kay J E, Holland M M, Jahn A. 2011. Inter-annual to multi-decadal arctic sea ice extent trends in a warming world. Geophysical Research Letters, 38(15): L15708

Kim B M, Son S W, Min S K, et al. 2014. Weakening of the stratospheric polar vortex by arctic sea-ice loss. Nature Communications, 5: 4646

Kuo Y H, Sokolovskiy S V, Anthes R A, et al. 2000. Assimilation of GPS radio occultation data for numerical weather prediction. Terrestrial, Atmospheric and Oceanic Sciences, 11(1): 157–186

Kuo Y H, Wee T K, Sokolovskiy S, et al. 2004. Inversion and error estimation of GPS radio occultation data. Journal of the Meteorological Society of Japan, 82(1B): 507–531

Kursinski E R, Hajj G A, Schofield J T, et al. 1997. Observing earth's atmosphere with radio occultation measurements using the global positioning system. Journal of Geophysical Research: Atmospheres, 102(D19): 23429–23465

Liu Yinghui, Key J R. 2003. Detection and analysis of clear-sky, low-level atmospheric temperature inversions with MODIS. Journal of Atmospheric and Oceanic Technology, 20(12): 1727–1737

Liu Yinghui, Key J R, Ackerman S A, et al. 2012. Arctic cloud macrophysical characteristics from CloudSat and CALIPSO. Remote Sensing of Environment, 124: 159–173

Liu Yinghui, Key J R, Schweiger A, et al. 2006. Characteristics of satellite-derived clear-sky atmospheric temperature inversion strength in the arctic, 1980–96. Journal of Climate, 19(19): 4902–4913

Melles M, Brigham-Grette J, Minyuk P S, et al. 2012. 2.8 million years of arctic climate change from Lake El'gygytgyn, NE Russia. Science, 337(6092): 315–320

Moradi I, Soden B, Ferraro R, et al. 2013. Assessing the quality of humidity measurements from global operational radiosonde sensors. Journal of Geophysical Research: Atmospheres, 118(14): 8040–8053

Schreiner W, Rocken C, Sokolovskiy S, et al. 2007. Estimates of the precision of GPS radio occultations from the COSMIC/FORMOSAT-3 mission. Geophysical Research Letters, 34(4): L04808

Stroeve J C, Markus T, Boisvert L, et al. 2014. Changes in arctic melt season and implications for sea ice loss. Geophysical Research Letters, 41(4): 1216–1225

Sun Bimin, Reale A, Seidel D J, et al. 2010. Comparing radiosonde and COSMIC atmospheric profile data to quantify differences among radiosonde types and the effects of imperfect collocation on comparison statistics. Journal of Geophysical Research: Atmospheres, 115(D23): D23104

Sun Bomin, Reale A, Schroeder S, et al. 2013. Toward improved corrections for radiation-induced biases in radiosonde temperature observations. Journal of Geophysical Research: Atmospheres, 118(10): 4231–4243

Titchner H A, Thorne P W, McCarthy M P, et al. 2009. Critically reassessing tropospheric temperature trends from radiosondes using realistic validation experiments. Journal of Climate, 22(3): 465–485

Wang B R, Liu X Y, Wang J K. 2013. Assessment of COSMIC radio occultation retrieval product using global radiosonde data. Atmospheric Measurement Techniques, 6(4): 1073–1083

Wickert J, Reigber C, Beyerle G, et al. 2001. Atmosphere sounding by GPS radio occultation: first results from CHAMP. Geophysical Research Letters, 28(17): 3263–3266

Xie F, Wu D L, Ao C O, et al. 2010. Super-refraction effects on GPS radio occultation refractivity in marine boundary layers. Geophysical Research Letters, 37(11): L11805

Yunck T P, Liu Chaohan, Ware R. 1999. A history of GPS sounding. Terrestrial, Atmospheric and Oceanic Science, 11(1): 1–20